European Journal of Human Genetics (2013) 21, 317–323

www.nature.com/ejhg

ARTICLE

FTO levels affect RNA modification and the transcriptome

Tea Berulava[1], Matthias Ziehe[2], Ludger Klein-Hitpass[3], Emil Mladenov[4], Jürgen Thomale[3], Ulrich Rüther[5] and Bernhard Horsthemke*[,1]

A block of single-nucleotide polymorphisms within intron 1 of the *FTO* (fat mass and obesity associated) gene is associated with variation in body weight. Previous works suggest that increased expression of *FTO*, which encodes a 2-oxoglutarate-dependent nucleic acid demethylase, leads to increased body weight, although the underlying mechanism has remained unclear. To elucidate the function of FTO, we examined the consequences of altered FTO levels in cultured cells and murine brain. Here we show that a knockdown of *FTO* in HEK293 cells affects the transcripts levels of genes involved in the response to starvation, whereas overexpression of *FTO* affects the transcript levels of genes related to RNA processing and metabolism. Subcellular localization of FTO further strengthens the latter notion. Using immunocytochemistry and confocal laser scanning microscopy, we detected FTO in nuclear speckles and – to a lesser and varying extent – in the nucleoplasm and nucleoli of HEK293, HeLa and MCF-7 cells. Moreover, RNA modification analyses revealed that loss of Fto affects the 3-methyluridine/uridine and pseudouridine/uridine ratios in total brain RNA. We conclude that altered levels of FTO have multiple and diverse consequences on RNA modifications and the transcriptome.
European Journal of Human Genetics (2013) **21,** 317–323; doi:10.1038/ejhg.2012.168; published online 8 August 2012

Keywords: FTO; RNA modifications; nuclear speckles; transcriptome

INTRODUCTION

Genome-wide association studies have revealed a strong association between a block of single-nucleotide polymorphisms (SNPs) in intron 1 of the fat mass and obesity-associated (*FTO*) gene, body mass index and other obesity-related traits in children and adults of different populations.[1–3] Stratigopoulos *et al*[4] have suggested that one of the SNPs (rs8050136) affects binding of the transcriptional regulator CUX1. By studying allelic expression levels in heterozygous individuals, we have found that the risk allele of the *FTO* gene makes more transcripts and have proposed that increased expression of the *FTO* gene leads to increased body weight.[5] This hypothesis is supported by the clinical findings in rare patients and in mouse models with an *FTO*/*Fto* mutation. Homozygous loss-of-function of *FTO* was reported to cause severe growth retardation and multiple malformations,[6] whereas a duplication of *FTO* was found to be associated with morbid obesity.[7] *Fto*-knockout mice[8] and mice with a missense mutation in exon 6[9] showed leanness, postnatal growth retardation and a higher metabolic rate. Mice with one or two additional copies of *Fto* had a gene-dosage-dependent increase in body weight.[10]

FTO is a member of non-heme Fe(II)- and α-ketoglutarate-dependent oxygenase superfamily and is found in vertebrates and green algea, but not in invertebrate animals, fungi and green plants.[11] By *in vitro* studies, FTO was shown to function as a demethylase with a strong preference for 3meU and 3meT in single-stranded RNA and DNA, respectively.[12,13] Han *et al*[14] have provided structural evidence for understanding the substrate specificity of FTO and have suggested that FTO may modify rRNA. Jia *et al* have shown that 6-methyladenosine in nuclear RNA is a major substrate of FTO, and Dominissini *et al* and Meyer Kate *et al* have mapped 6-methyladenosine in mRNA.[15–17] Others have suggested that FTO might function as transcription factor.[18]

For elucidating the function of FTO, we have determined the subcellular localization of FTO and the effect of FTO dosage on RNA expression profiles and RNA modification levels.

MATERIALS AND METHODS

Constructs

An untagged full-length *FTO* cDNA clone for native protein expression was purchased from Origene (Rockville, MD, USA. Cat. No SC315786). The ORF with its original Kozak sequence and part of the 3′UTR (including the first two polyadenylation signal sequences) was subcloned into the NotI site of pcDNA5/FRT/TO to generate pcDNA/FRT/TO_FTO. The cDNA was fully sequenced to exclude any mutations. pcDNA5/FRT/TO, pOG44 expressing Flp recombinase and pcDNA5/FRT/TO_GFP (as a positive control) were obtained from Invitrogen (Carlsbad, CA, USA).

Cell culture

All cells (HeLa, MCF-7, HEK293, Flp-In 293 T-Rex and its derivates) used in this study were cultured in DMEM medium supplemented with FCS 10% and PenStrep 1% in a humidified incubator at 37 °C supplied with 5% CO_2. Blasticidin, zeocin and hygromycin were used as selective antibiotics at different stages for Flp-In 293 T-Rex and its derivates.

[1]Institut für Humangenetik, Universitätsklinikum Essen, Essen, Germany; [2]Department of Analytical and Environmental Chemistry, Humboldt-Universität zu Berlin, Berlin, Germany; [3]Institut für Zellbiologie (Tumorforschung), Universitätsklinikum Essen, Essen, Germany; [4]Institut für medizinische Strahlenbiologie, Universitätsklinikum Essen, Essen, Germany; [5]Institut für Entwicklungs- und Molekularbiologie der Tiere (EMT) Heinrich-Heine-Universität, Düsseldorf, Germany
*Correspondence: Professor B Horsthemke, Institut für Humangenetik, Universitätsklinkum Essen, Hufelandstrasse 55, Essen 45122, Germany. Tel: +49 201 7234556; Fax: +49 201 7235900; E-mail: bernhard.horsthemke@uni-due.de
Received 6 February 2012; revised 11 July 2012; accepted 13 July 2012; published online 8 August 2012

Generation of *FTO*-overexpressing cell lines

To generate *FTO*-overexpressing cell lines, we used the Flp-In 293 T-Rex system, which allows tetracycline-inducible expression of a gene of interest (Invitrogen). Cells were cotransfected with pcDNA/FRT/TO_FTO (or pcDNA5/FRT/TO_GFP as a positive control) and pOG44 at 9:1 ratio with Fugene reagent (Roche, Basel, Switzerland). Empty pcDNA/FRT/TO was used as a negative control. Three independent single-cell-derived clones (FTO1_C1, FTO2_D4 and FTO3_A3) were selected for further experiments. All cell lines were checked for β-galactosidase activity. Clones FTO1_C1 and FTO2_D4, but not clone FTO3_A3, showed increased FTO expression upon induction. As an inducing agent doxycycline was used, as it has several advantages over the tetracycline (www.invitrogen.com).

siRNA transfection

Unmodified Flp-In 293 T-Rex cells were used for *FTO*-knockdown experiments. Commercially available siRNA designed for *FTO* was purchased from Origene (Cat. No SR312322). The kit contained three different siRNAs, two aimed at the 3′UTR and one at the coding sequence. Universal scrambled negative control siRNA absent in human, mouse and rat genomes was also provided with the kit. To evaluate efficiency of transfection, Cy3-labeled control siRNA (Origene, Cat. No SR30002) was used. As a transfection reagent, lipofectamine 2000 (Invitrogen, Carlsbad, CA, USA) was used.

Transfections were performed followed by standard protocols at 10 nM concentration of siRNAs. Briefly, cells were plated 1 day before transfection. On the day of transfection, the medium was changed, and 2 h later silencing complexes (siRNAs and lipofectamine in OPTIMem, Invitrogen) were added in a drop-like manner.

RNA preparation

For *FTO*-knockdown and -overexpression cells, RNeasy mini kit (Qiagen, Hilden, Germany) was used to prepare total cellular RNA. DNase I treatment was performed twice for each sample, first on spin columns during extraction, and afterwards in solution of eluted RNA. After the second DNase I treatment, all samples were cleaned up with the RNaesy mini kit. RNA from brain of *Fto*-deficient[8] and wild-type mice was extracted with miRNeasy kit (Qiagen) following the instruction of the manufacturer. Small RNA fraction was eluted with the miniElute kit (Qiagen). Using this approach, two fractions of RNA was prepared: large RNAs above 200 nt (mRNA with ribosomal RNAs) and small RNAs – $<$200 nt (enriched with miRNAs, transferring RNAs, 5 S and 5.8 S rRNAs). Large RNA fraction was treated with DNase I twice, like total cellular RNA.

Protein extraction and western blotting

Briefly, cells were washed, resuspended in PBS and centrifugated for 2 min at 13 000 r.p.m. Pellets were resuspended in the appropriate volume of WCE buffer (30 mM Tris-HCl, pH 8, 0.42 M NaCl, 0.5 mM EDTA and 20% glycerol) supplemented with protease/phosphatase inhibitors (Roche) and sonicated using a Branson Sonifier (Branson Ultrasonics, Danbury, CT, USA) at constant power with the following settings: duty cycler 40–50 and output control 2.5. Samples were rested at 4 °C in between to cool down. Insoluble material was pelleted by centrifugation for 15 min at 4 °C, 13 000 r.p.m. The protein concentration was measured by standard Bradford assay.

Proteins were separated by SDS/PAGE (10% gel), followed by blotting and detection with enhanced chemiluminescence reagent (Thermo Fisher Scientific, Waltham, MA, USA). The primary antibodies used were mouse and rabbit anti-FTO (Abcam, Cambridge, UK; Epitomics, Burlingame CA, USA) and rabbit anti-GAPDH (Cell Signaling Technology, Danvers, MA, USA). Secondary antibodies were goat anti-mouse and anti-rabbit HRP (horseradish peroxidase)-conjugated antibodies (Thermo Fisher Scientific).

Microarray analyses

For microarray analyses, we used the Affymetrix GeneChip platform employing the Express Kit protocol for sample preparation and microarray hybridization (Affymetrix, Santa Clara, CA, USA). Total RNA (200 ng) was converted into biotinylated cRNA, purified, fragmented and hybridized to HG-U133Plus_2.0 microarrays (Affymetrix). The arrays were washed and stained according to the manufacturer's recommendation and finally scanned in a GeneChip scanner 3000 (Affymetrix).

Array images were processed to determine signals and detection calls (Present, Absent and Marginal) for each probe set using the Affymetrix GCOS1.4 software (MAS 5.0 statistical algorithm). Arrays were scaled across all probe sets to an average intensity of 1000 to compensate for variations in the amount and quality of the cDNA samples and other experimental variables of non-biological origin. Pairwise comparisons of experiments (*FTO* overexpression and knockdown) *versus* control (not induced and scrambled siRNA treated) samples were carried out with GCOS1.4, which calculates the significance (change *P*-value) of each change in gene expression based on a Wilcoxon ranking test. To limit the number of false positives, we restricted further target identification to those probe sets that received at least one present detection call in the treated/control pair. As many genes are represented by more than one probe set, most likely reflecting different transcripts from the same region, the lists of deregulated genes in FTO-overexpressing and -depleted cells (Supplementary Tables S1 and S2) were generated based on identical probe sets only.

RNA hydrolysis

RNA samples were hydrolyzed as described.[19] Briefly, RNAs were denaturated at 100 °C and rapidly chilled down in ice water. Then 1/10 of volume 0.1 M ammonium acetate and 2 units for 20 μg of RNA nuclease P1 (Sigma-Aldrich, St Louis, MO, USA) were added. Solutions were incubated at 45 °C for 2 h. Hydrolysis was continued further by adding venom phosphodiesterase (Sigma-Aldrich) at 37 °C for another 2 h. Finally, digested ribonucleotides were dephosphorylated to ribonucleosides by alkaline phosphatase (Fermentas, Thermo Fisher Scientific). The solutions were analyzed by HLPC-MS.

HPLC-MS

Digested RNA solutions were diluted in 2′-deoxycytidine 5′-monophosphate (pdC) containing deionized water to appropriate concentrations for measurements. pdC was used as an internal standard with the same amount in all samples and standard solutions. All calculated areas were traced back to the pdC signal to compensate sensitivity fluctuations during the measurements.

All samples were analyzed using an Agilent 1200 HPLC system (Agilent Technologies, Santa Clara, CA, USA) coupled to a LTQ iontrap (Thermo Scientific, Bremen, Germany) in positive electrospray ionization mode. Samples were separated using an Atlantis T3 reversed phase column (1 × 150 mm, 3 μm) (Waters Corporation, Milford, MA, USA). Quantification of nucleosides was performed in single-reaction monitoring mode based on the nucleoside to base ion mass transitions shown in Supplementary Table S5. Each sample was measured at least three times. Calculations of the ratios of modified to unmodified nucleoside were performed in comparison with standard curves. Standards were analyzed before, between and after each batch. Parameters for HLPC and MS are given in the end of Supplementary Table S5.

Real-time PCR

RNA was reverse transcribed into cDNA using GeneAmpl RNA PCR Kit and random hexamers (Applied Biosystems, Foster City, CA, USA). Dual color real-time PCR was performed on LightCycler 480 System using FAM-labeled probes from Universal ProbeLibrary and Yellow-555-labeled universal reference GAPDH probe (Roche). LightCycler 480 probes master was used in reaction (Roche). Primers and probes are given in the Supplementary Table S6.

Immunocytochemistry and microscopy

Immunocytochemistry was performed as described.[20] Briefly, cells were seeded on sterile cover slips 1 day before immunostaining. The whole procedure was performed at room temperature. Cells were washed with PBS and fixed in methanol for 10 min, again washed with PBS and equilibrated in I buffer (10 mM Tris pH 7.5, 100 mM NaCl, supplemented with 0.05% Tween 20 and 1% BSA) for at least 30 min. Primary antibodies used for immunoflueresence staining for FTO, fibrillarin, PML, COIL and SC35 were from mouse and rabbit (Abcam; Epitomics). Secondary antibodies were labeled either with Cy3 (goat anti-mouse and anti-rabbit, Dianova GmbH, Hamburg, Germany) or

Alexa Fluor 488 (goat anti-mouse and anti-rabbit, Invitrogen). The dilutions 1:300 and 1:600 in I buffer were used for Cy3- and Alexa Fluor 488-labeled antibodies, respectively. Dilutions for primary antibodies were in the range from 1:100 to 1:1000. Cover slips were washed in between with I buffer, stained with DAPI and mounted on microscope slides in Antifade gold medium.

RNA-fluorescence *in situ* hybridization (FISH)

FISH probes were prepared by digoxigenin-nick translation (Roche) of PCR products for MALAT1 and NEAT1. Cells seeded on cover slips 1 day before the experiment were washed in PBS, incubated in CSK buffer for 5 min, and fixed in 4% paraformladehyde in PBS for 10 min in ice water. Later slides were washed in 70% ethanol, dehydrated in higher concentrated ethanol and hybridized to denaturated probes at 37 °C overnight in humidified chamber. For colocalization analyses, before applying primary rabbit anti-digoxigenin and mouse anti-FTO antibodies, cells were again fixed with 2% paraformaldehyde in PBS for 15 min at room temperature. Secondary antibodies used were anti-rabbit Alexa Flour 488 (Invitrogen) and anti-mouse Cy3 (Dianova GmbH). Finally cells were stained with DAPI and mounted in antifade gold on the microscope slides.

Confocal laser microscopy

Immunofluorescence-stained cells were visualized by using a Leica TCS SP5 confocal microscope with a 63 × /1.4 oil immersion Leica objective (Leica Microsystems, Wetzlar, Germany). In order to avoid cross talk between different channels, bidirectional scans were applied in a sequential scan modus with predefined settings. Mostly, a resolution of 1024 × 1024 and a zoom factor of 2 were set, resulting in a pixel size of about 100 nm. For each slide, at least two fields were scanned at different *z*-sections with 0.5-μm steps within a *z*-stack. After each scan, three-dimensional data sets (LIF files) and maximum intensity projection TIFF images of the field scanned were generated.

RESULTS

FTO overexpression

For controlled and homogeneous overexpression of *FTO* in a defined cell type, we have generated stable cell lines exhibiting tetracycline-inducible expression *FTO*. For this, we have integrated the *FTO* cDNA into the single FRT site of Flp-In 293T-Rex cells (Invitrogen). We intentionally avoided any tag to ensure proper function of the transgene-encoded FTO. Two independent (single cell derived) clones (FTO1_C1 and FTO2_D4) showing overexpression of *FTO* were selected. qPCR confirmed 8–10-fold overexpression upon induction after 24 and 48 h. Semiquantitative western blot showed 3–5 times more FTO protein in induced cells compared with uninduced controls. By immunocytochemical analysis, FTO was found to be located mainly in nucleus (Figure 1a-c). Induced cells did not have any obvious phenotype.

For finding out whether increased levels of FTO affected steady-state levels of specific mRNAs, we isolated RNA (>200 nt) from two independent clones after 48 h of FTO induction, and analyzed it on Affymetrix U133 plus2.0 microarrays. We compared transcript levels in uninduced and induced clones FTO1_C1 and FTO2_D4 and selected genes that showed changed transcript levels in both clones (Supplementary Table S1). Of those, the great majority (95%) showed increased transcripts levels. Although the fold changes were small (see also the confirmatory qRT-PCR analyses for *MALAT1* and *RBM25* in Supplementary Figure S3A), gene set enrichment analyses identified 54 GO subcategories with the following top five: 'RNA splicing' ($P=0.00033$), 'mRNA metabolic process' ($P=0.00075$), 'nucleic acid metabolic process' ($P=0.00075$), 'nucleobase, nucleoside, nucleotide and nucleic acid metabolic process' ($P=0.00077$) and 'RNA splicing, via transesterification reactions' ($P=0.0023$) (Supplementary Table S2). The hint to RNA processing was further strengthened by the subcategory 'spliceosome' from the KEGG database ($P=0.0017$). Overrepresentation of genes with RNA-recognition motifs and KH domains was found for both clones ($P=0.0016$ and $P=0.011$, respectively).

As shown in other experiments, doxycycline itself had no effect on the transcriptome.[21] Using the same system, Grosser and Horsthemke (unpublished) overexpressed TET1 and TET3, which also belong to the non-heme Fe(II)- and α-ketoglutarate-dependent oxygenase superfamily. In contrast to FTO, which demethylates *N*-methyl ribonucleosides such as 3-methyl-uridine and 6-methyl-adenosine,

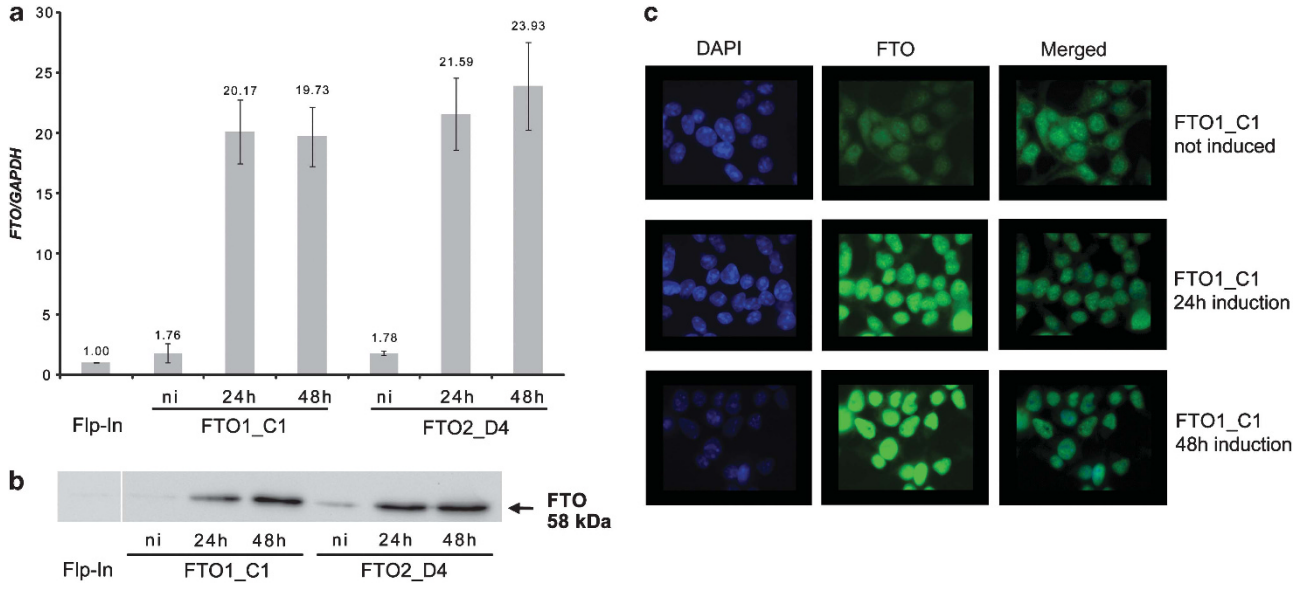

Figure 1 Overexpression of *FTO* in Flp-In 293 T-Rex cells. (**a**) Real-time PCR analyses of FTO1_C1 and FTO2_D4 clones. Means ± SD of three independent analyses using duplicates are given. ni, not induced, Flp-In, unmodified Flp-In 293 T-Rex cells. (**b**) Western blot analysis demonstrated overexpression of FTO protein in both clones. (**c**) Immunostaining using an antibody against FTO showed that overexpressed FTO is present in the nucleus. In addition, dot-like enrichment of FTO on evenly distributed nucleoplasmic background is visible.

TET1 and TET3 oxygenate 5-methyl-desoxycytidine. Overexpression of these two genes did not affect transcripts involved in RNA processing and metabolism. Thus, the observed effects of FTO overexpression on the gene sets related to RNA metabolism and processing are highly specific.

FTO knockdown

For finding out whether decresased levels of FTO affected steady-state levels of specific mRNAs, we knocked down *FTO* in Flp-In 293 T-Rex cells by transient transfection with *FTO*-specific siRNA. As a control, scrambled siRNA was used. After 48 h, *FTO* mRNA levels were reduced to <20% and FTO protein levels were reduced to <40% (Figure 2a and b). Cells were viable and showed no obvious change in their phenotype. RNA was extracted after 48 h of transfection from two biological replicas and analyzed on Affymetrix U133 plus2.0 microarrays. A total of 183 genes showed changed expression in both experiments (Supplementary Table S3). Of those, the majority (78%) showed decreased levels of transcripts. Gene set analyses revealed overrepresentation of genes in two GO subcategories: 'cellular response to starvation' ($P=0.019$) and 'response to starvation' ($P=0.036$) (Supplementary Table S4). For validation of the microarray data, we perfomed qRT-PCR analyses for *MALAT1*, *LIN28B*, *RAB12*, *GNG12* and *ATG5*. Except for *ATG5*, we could demonstrate decreased transcripts levels in *FTO*-knockdown cells (Supplementary Figure S3B). Reinspection of the microarray data on *MALAT1* showed that most of the probe sets indicated reduced levels, but the gene had not met our most stringent filter criteria (GSE33870).

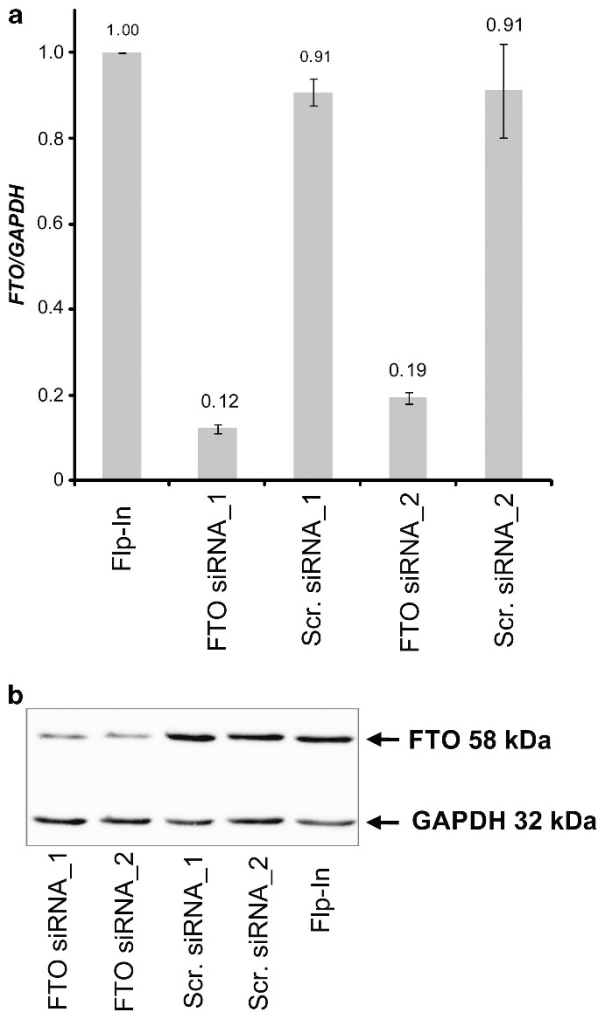

Figure 2 Knockdown of *FTO* in Flp-In 293 T-Rex cells. (**a**) qPCR showed decreased FTO mRNA levels in both *FTO*-specific siRNA transfections. Three independent experiments were performed (mean values with SD are depicted). (**b**) Reduced protein levels were revealed by western blot.

Subcellular localization of FTO

As the expression profile of *FTO*-overexpressing cells pointed to RNA processing, which occur in specific compartments of the cell nucleus, we used immunocytochemistry to determine the subcellular localization of FTO. In the beginning of the work, *FTO*-overexpressing cells were examined to see whether overexpressed FTO is still imported into nucleus. We observed that FTO (i) is mostly of nuclear localization and (ii) enriched at discrete spots on the background of even nucleoplasmic distribution (Figure 1c). We extended the analysis to different cell types (HEK293, HeLa and MCF-7) and confirmed that in all cell types FTO accumulates in dot-like structures, whereas the intensity of nucleoplasmic staining appeared to vary between different cells (Supplementary Figure S1). In particular, HeLa, HEK293 as well as unmodified and transgenic Flp-In 293 T-Rex cells showed a rather similar pattern—enrichment in dot-like structures and significant and homogeneous nucleoplasmic signal, whereas MCF-7 cells, which divide more slowly, showed a different picture:FTO is concentrated at particular spots, but nucleoplasm is less intensively stained. Another interesting observation was the presence of FTO in nucleoli in all investigated cell types. Moreover, in MCF-7 cells nucleoli appeared to be enriched with FTO relative to the surrounding nucleoplasm. Of note, when FTO expression was induced, nucleoli retained their basic level of FTO.

For identification of the dot-like nuclear structures enriched with FTO, we analyzed HeLa and MCF-7 cells by immunocytochemistry and FISH. First, we checked for localization of FTO to nuclear speckles and paraspeckles, because speckles serve for storage and/or modification of splicing factors, and paraspeckles serve for RNA editing and nuclear retention. In addition, the microarray data had shown changed transcript levels of *MALAT1* and *NEAT1*, which are long non-coding RNAs found in speckles and paraspeckles, respectively. As the best antibodies for FTO and SC35 (protein marker for nuclear speckles) were from mouse, we decided to combine RNA-FISH for MALAT1 with immunostaining for FTO. For paraspeckles, we used RNA-FISH for NEAT1, because none of antibodies for paraspeckle-specific protein (PSPC1) worked well in our hands.

Confocal laser microscopy revealed that FTO is enriched in nuclear speckles but not paraspeckles (Figure 3). The degree of colocalization between nuclear speckles and FTO was much higher in MCF-7 cells than in HeLa cells, consistent to the observation that in HeLa cells a significant proportion of FTO is distributed throughout the nucleoplasm.

We also checked whether FTO colocalizes with other known nuclear bodies. There was no enrichment of FTO at Cajal and PML bodies. However, a striking observation was that when cells were stained with anti-FTO and anti-PML antibodies, FTO signal from nucleoli appeared to be much stronger than in cells stained with anti-FTO only (Supplementary Figure S2).

Modification of brain RNA in wild-type and *Fto*-knockout mice

As shown by Gerken *et al*,[12] 3-methyl-uracil and 3-methyl-thymine in single-stranded RNA and DNA, respectively, are the preferred *in vitro* substrates of mouse and human Fto/FTO. Given that RNA

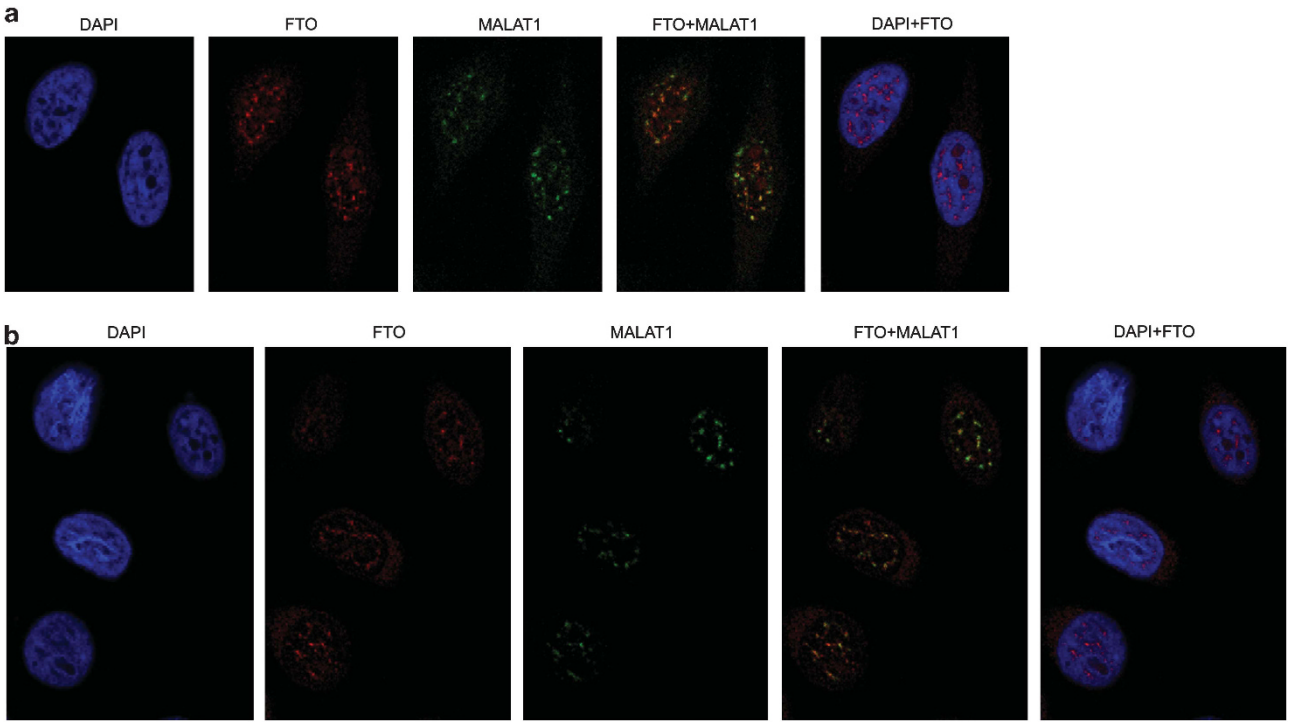

Figure 3 Intranuclear localization of FTO in Hela (**a**) and MCF-7 cells (**b**). RNA-FISH for the non-coding long RNA MALAT1, which is a component of nuclear speckles, and immunostaining for FTO protein showed that FTO is enriched at nuclear speckles. Note that FTO is also present in nucleoli. DNA was counterstained with DAPI.

(in particular ribosomal RNA) is abundant in cells and mainly single-stranded, Han *et al*[14] have suggested that RNA may be the primary substrate of FTO. Our expression profile and subcellular localization studies support this view and prompted us to examine the ratio of modified to unmodified ribonucleosides. We chose mouse brain, because (i) *Fto* expression is highest in brain, and (ii) *Fto*-knockout mice (Fischer *et al*[8]) completely lack Fto. Thus, any effect should be most obvious and functionally relevant.

Total RNA from whole brains of wild-type and $Fto^{-/-}$ mice was prepared and separated into two fractions: large RNAs (>200 bases) and small (< 200 bases) RNAs. The first fraction contains mainly rRNA, whereas the second fraction contains mainly tRNAs. Samples were digested enzymatically and analyzed by high-performance liquid chromatography on an Agilent 1200 system coupled to an LTQ iontrap (HPLC-MS). For exemplary LC-MS traces, see Supplementary Figure S4. Each preparation of sample RNA was measured at least three times. The following ribonucleosides, which have been shown as substrates and reaction products, respectively, of FTO[12,15] were measured: 3-methyluridine (3meU), uridine (U), 6-methyladenine (6meA), adenine (A), 3-methylcytidine (3meC) and cytidine (C). We also included pseudouridine (ΨU), because it has been shown that pseudouridinylation is inhibited by 3-methylation of uridine.[22] Calculations of the ratios of modified and unmodified nucleosides were done relative to standard curves.

We analyzed four $Fto^{-/-}$ animals (two females and two males) against five wild-type mice (three females and two males) (Figure 4). In the large RNA fraction, the ratio of 3meU/U in female $Fto^{-/-}$ mice was 33% higher than in wild-type animals. In males, the ratios were also significantly different and in the same direction (+14%), although the difference was less prominent. The ratio of ΨU/U in $Fto^{-/-}$ animals compared with their wild-type littermates was significantly lower, although the change was small: −17% for females and −3% for males. The direction of change was the same for both sexes. The 6meA/A and 3meC/C ratios did not differ from wild-type mice, neither in male nor female animals (0.93 ± 0.11 and 1.11 ± 0.20 for N6meA/A, 0.96 ± 0.04 and 1.04 ± 0.10 for 3meC/C, for male and female *Fto*-knockout mice, respectively. Normalized means ± SD are given). In contrast to the large RNA fraction, there were no significant changes in the small RNA fraction (data not shown).

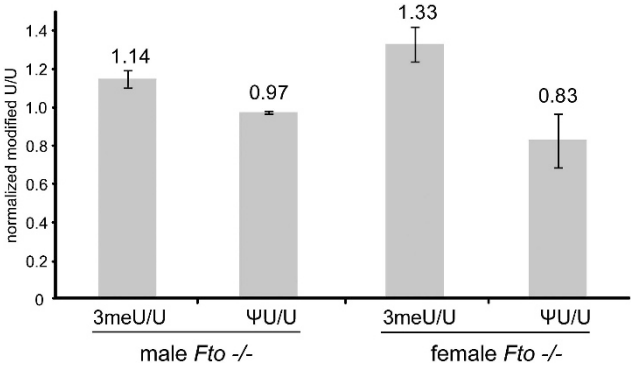

Figure 4 Effect of loss of FTO on normalized 3-methyluridine/uridine and pseudouridine/uridine ratios in total brain RNA. Each RNA sample was measured at least three times. The mean ratios of modified/unmodified U in wild-type animals were set to 1 and used to normalize the ratios in $Fto^{-/-}$ mice. Mean ± SD are given.

DISCUSSION

In the present study, we have examined the consequences of altered FTO levels in cultured cells and murine brain. We have found that

overexpression of *FTO* in HEK293 predominantly changed the steady-state mRNA levels of genes involved in RNA processing and metabolism, whereas a knockdown of *FTO* changed the mRNA levels of genes involved in cellular response to starvation. Moreover, we could demonstrate that FTO is present in nuclear speckles and—to a lesser and varying extent—in the nucleoplasm and nucleoli. By measuring ratios of modified and unmodified ribonucleosides in total RNA from the brain of wild-type and *Fto*-knockout mice, we found changes in the levels of 3-methyluridine and pseudouridine. We conclude that altered levels of FTO have multiple and diverse consequences.

As we measured steady-state levels of transcripts, it is difficult to identify the cause for the observed changes of the transcriptome. In general, changed transcripts levels can be the result of changed rates of RNA transcription, processing or degradation. Wu *et al* have suggested that FTO might serve as a transcription factor. Although we cannot exclude this possibility, we consider this as unlikely, because (i) FTO is an enzyme, (ii) overexpression of *FTO* had little effects on the transcriptome after 24 h (data not shown) and (iii) the observed fold changes after 48 h were—although significant—rather small. If there is an effect of altered FTO levels on transcription rates, it is likely to be indirect. An indirect effect means that a change in FTO levels disturbs the cellular system and elicits evasive or compensatory mechanisms through autoregulatory feedback loops. It is remarkable that overexpression of FTO results in increased levels of transcripts coding for proteins involved in RNA processing and metabolism, and that RNA processing factors and FTO colocalize within the nucleus (see below). How the change of these transcripts is linked to increased body weight is unclear.

There are also arguments why altered levels of FTO might affect RNA processing and stability. FTO has been reported to demethylate single-stranded RNA *in vitro* and *in vivo*. Although the biological relevance of RNA methylation is not completely understood, the well described and site-specific localization of different modifications implies significant biological role.[16,17] Most likely, these modifications affect RNA structure, stability, accessibility to binding factors and/or processing. In agreement with these suggestions, recent studies found that 6-methyladenosine is enriched at miRNA-binding sites[17] and possibly affects alternative splicing.[16] Intriguingly, MALAT1, the long non-coding RNA that regulates alternative splicing and is associated with nuclear speckles harboring FTO (see below and Jia *et al*[15]), has been reported to have a high degree of 6-methyladenine.[17] Taken together, this finding and our expression data suggest that the steady-state levels of *MALAT1* may be controlled by FTO-dependent demethylation of MALAT1.

The knockdown of *FTO* affected the mRNA levels of other genes. This may not be too surprising, because overexpression of *FTO* in mice affects body weight only, whereas loss-of-function mutations in mice[8,9] and humans[6] did not only result in reduced body weight but also other defects. We found significant changes in the GO subcategory: 'cellular response to starvation'. Interestingly, expression of the *FTO* itself has been reported to be regulated by the nutritional state of the cell.[23] The GO subcategory 'cellular response to starvation' includes genes specific for autophagy (for example *ATG5* and *BECN1*). Recently, several links between body weight regulation and autophagy in the liver, adipose tissue and hypothalamic cells have been established.[24–26] Although we were not able to verify reduced transcripts levels of the *ATG5* gene by qRT-PCR, the possible link between autophagy and FTO function may merit further examination. In view of the link between autophagy and ciliary function (see eg, Huber *et al*[27]), it is worth noting that overexpression and depletion of FTO affected transcript levels of several genes involved in ciliary function (indicated by * in Supplementary Tables S1 and S3).

Our subcellular localization studies revealed that FTO is enriched at nuclear speckles. This observation confirms the findings of Jia *et al*.[15] Nuclear speckles are thought to serve for the storage/modification of pre-mRNA splicing factors. They contain transcription factors, 3′-end RNA processing factors, translation regulation factors and the large subunit of RNA polymerase II.[28,29] Jia *et al* have shown also that the inhibition of transcription changes the nucleoplasmic distribution of FTO, which becomes more concentrated at speckles. Of note, we observed different pattern of nucleoplasmic FTO staining in cells with different proliferation rates.

Apart from speckles, we also identified nucleoli as a subnuclear structure containing FTO. Nucleoli are the site of rRNA transcription and procession. The presence of FTO in nucleoli suggests that FTO might be involved in rRNA modification. In fact, we found an increased ratio of 3meU/U in total RNA from $Fto^{-/-}$ brains compared with wild-type brains. As total RNA consists mainly of rRNA, we believe that the observed changes are mainly owing to changes in the modification of rRNA. Our finding is in line with the fact that *in vitro* 3meU is the preferred substrate of FTO.[12] We did not observe any significant changes of the 6meA/A and 3meC/C ratios in the large RNA fraction. This may reflect the fact that 6meA and 3meC are poor substrates of FTO[12] or that the RNA molecules containing these modifications are underrepresented in total RNA, so that any changes are below the detection level of our analyses. In fact, Jia *et al* and Meyer Kate *et al* have recently reported that 6meA in mRNA is a substrate of FTO. Taken together, our study and the studies by Jia *et al*[15] and Meyer Kate *et al*[17] show that FTO has multiple RNA substrates.

Interestingly, we observed a decreased ratio of ΨU/U in FTO-deficient mice. As 3-methylation of uridine inhibits its H/ACA snoRNA-guided isomerization to psesudouridine,[22] the observed decrease in the ΨU/U ratio in FTO-deficient mice is in line with the increased 3meU/U ratio. Pseudouridine has recently been reported to affect translation efficiency,[30] and ribosomal activity has been linked to obesity.[31] Another interesting study has demonstrated that pseudouridylation of the spliceosomal small nuclear RNA U2 is affected by nutrition.[32] We have not observed any changes in uridine modifications in the small RNA fraction, but our RNA preparation is probably enriched with transferring RNAs so that changes affecting snRNAs may have gone undetected.

In summary, the work by us and others suggests that changes in FTO dosage, which affect body weight, has multiple effects. Altered FTO levels appear to affect different modifications (6mA, 3meU and – indirectly – ΨU) in different classes of RNA (mRNA and probably rRNA) as well as the mRNA level of genes belonging to specific functional categories (RNA processing and metabolism). In view of the different RNA modifications, it will be of utmost importance to identify the endogenous RNA targets and the relevant tissue(s).

CONFLICT OF INTEREST

The authors declare no conflict of interest.

ACKNOWLEDGEMENTS

We thank Professor G Iliakis for providing access to the confocal laser microscope and Professor M Linscheid for providing equipment and helpful suggestions. We are grateful to one of the anonymous reviewers for pointing out the genes related to ciliary function. We are thankful to Christian Grosser for sharing his data. This work was supported by the Bundesministerium für Bildung und

Forschung (NGFN plus 01GS0820) and Deutsche Forschungsgemeinschaft (LI309/19-1, LI309/30-2).

Accession code: Miccroarray data generated by hybridization of RNA from both FTO1_C1 and FTO2_D4 clones with and without induced expression as well as from *FTO* siRNA- and scrampled siRNA-treansfected cells can be obtained from Gene Expression Omnibus (GSE33870). URL: GeneTrail gene set analysis tool at http://genetrail.bioinf.uni-sb.de/.

1 Dina C, Meyre D, Gallina S *et al*: Variation in FTO contributes to childhood obesity and severe adult obesity. *Nat Genet* 2007; **39**: 724–726.
2 Frayling TM, Timpson NJ, Weedon MN *et al*: A common variant in the FTO gene is associated with body mass index and predisposes to childhood and adult obesity. *Science* 2007; **316**: 889–894.
3 Scuteri A, Sanna S, Chen WM *et al*: Genome-wide association scan shows genetic variants in the FTO gene are associated with obesity-related traits. *PLoS Genet* 2007; **3**: e115.
4 Stratigopoulos G, LeDuc CA, Cremona ML *et al*: Cut-like homeobox 1 (CUX1) regulates expression of the fat mass and obesity-associated and retinitis pigmentosa GTPase regulator-interacting protein-1-like (RPGRIP1L) genes and coordinates leptin receptor signaling. *J Biol Chem* 2011; **286**: 2155–2170.
5 Berulava T, Horsthemke B: The obesity-associated SNPs in intron 1 of the FTO gene affect primary transcript levels. *Eur J Hum Genet* 2010; **18**: 1054–1056.
6 Boissel S, Reish O, Proulx K *et al*: Loss-of-function mutation in the dioxygenase-encoding FTO gene causes severe growth retardation and multiple malformations. *Am J Hum Genet* 2009; **85**: 106–111.
7 van den Berg L, de Waal HD, Han JC *et al*: Investigation of a patient with a partial trisomy 16q including the fat mass and obesity associated gene (FTO): fine mapping and FTO gene expression study. *Am J Med Genet A* 2010; **152A**: 630–637.
8 Fischer J, Koch L, Emmerling C *et al*: Inactivation of the Fto gene protects from obesity. *Nature* 2009; **458**: 894–898.
9 Church C, Lee S, Bagg EA *et al*: A mouse model for the metabolic effects of the human fat mass and obesity associated FTO gene. *PLoS Genet* 2009; **5**: e1000599.
10 Church C, Moir L, McMurray F *et al*: Overexpression of Fto leads to increased food intake and results in obesity. *Nat Genet* 2010; **42**: 1086–1092.
11 Robbens S, Rouze P, Cock JM *et al*: The FTO gene, implicated in human obesity, is found only in vertebrates and marine algae. *J Mol Evol* 2008; **66**: 80–84.
12 Gerken T, Girard CA, Tung YC *et al*: The obesity-associated FTO gene encodes a 2-oxoglutarate-dependent nucleic acid demethylase. *Science* 2007; **318**: 1469–1472.
13 Jia G, Yang CG, Yang S *et al*: Oxidative demethylation of 3-methylthymine and 3-methyluracil in single-stranded DNA and RNA by mouse and human FTO. *FEBS Lett* 2008; **582**: 3313–3319.
14 Han Z, Niu T, Chang J *et al*: Crystal structure of the FTO protein reveals basis for its substrate specificity. *Nature* 2010; **464**: 1205–1209.
15 Jia G, Fu Y, Zhao X *et al*: N6-methyladenosine in nuclear RNA is a major substrate of the obesity-associated FTO. *Nat Chem Biol* 2011; **7**: 885–887.
16 Dominissini D, Moshitch-Moshkovitz S, Schwartz S *et al*: Topology of the human and mouse m6A RNA methylomes revealed by m6A-seq. *Nature* 2012; **485**: 201–206.
17 Meyer Kate D, Saletore Y, Zumbo P *et al*: Comprehensive analysis of mRNA methylation reveals enrichment in 32 UTRs and near stop codons. *Cell* 2012; **149**: 1635–1646.
18 Wu Q, Saunders RA, Szkudlarek-Mikho M *et al*: The obesity-associated Fto gene is a transcriptional coactivator. *Biochem Biophys Res Commun* 2010; **401**: 390–395.
19 Crain PF: Preparation and enzymatic hydrolysis of DNA and RNA for mass spectrometry. *Methods Enzymol* 1990; **193**: 782–790.
20 Wawrzik M, Unmehopa UA, Swaab DF *et al*: The C15orf2 gene in the Prader-Willi syndrome region is subject to genomic imprinting and positive selection. *Neurogenetics* 2010; **11**: 153–161.
21 Neumann LC, Markaki Y, Mladenov E *et al*: The imprinted NPAP1/C15orf2 gene in the Prader–Willi syndrome region encodes a nuclear pore complex associated protein. *Hum Mol Genet* 2012 ; e-pub ahead of print 3 July 2012; doi:10.1093/hmg/dds228.
22 Zhou J, Liang B, Li H: Functional and structural impact of target uridine substitutions on the H/ACA ribonucleoprotein particle pseudouridine synthase. *Biochemistry* 2010; **49**: 6276–6281.
23 Cheung MK, Gulati P, O'Rahilly S *et al*: FTO expression is regulated by availability of essential amino acids. *Int J Obes* 2012; ; e-pub ahead of print 22 May 2012; doi: 10.1038/ijo.2012.77.
24 Kaushik S, Rodriguez-Navarro JA, Arias E *et al*: Autophagy in hypothalamic AgRP neurons regulates food intake and energy balance. *Cell Metab* 2011; **14**: 173–183.
25 Rabinowitz JD, White E: Autophagy and metabolism. *Science* 2010; **330**: 1344–1348.
26 Zhang Y, Goldman S, Baerga R *et al*: Adipose-specific deletion of autophagy-related gene 7 (atg7) in mice reveals a role in adipogenesis. *Proc Natl Acad Sci USA* 2009; **106**: 19860–19865.
27 Huber TB, Walz G, Kuehn EW: mTOR and rapamycin in the kidney: signaling and therapeutic implications beyond immunosuppression. *Kidney Int* 2011; **79**: 502–511.
28 Spector DL, Lamond AI: Nuclear speckles. *Cold Spring Harb Perspect Biol* 2011; **3**: a000646.
29 Tripathi V, Ellis JD, Shen Z *et al*: The nuclear-retained noncoding RNA MALAT1 regulates alternative splicing by modulating SR splicing factor phosphorylation. *Mol Cell* 2010; **39**: 925–938.
30 Jack K, Bellodi C, Landry DM *et al*: rRNA pseudouridylation defects affect ribosomal ligand binding and translational fidelity from yeast to human cells. *Mol Cell* 2011; **44**: 660–666.
31 Estornell E, Cabo J, Barber T: Protein synthesis is stimulated in nutritionally obese rats. *J Nutr* 1995; **125**: 1309–1315.
32 Wu G, Xiao M, Yang C *et al*: U2 snRNA is inducibly pseudouridylated at novel sites by Pus7p and snR81 RNP. *EMBO J* 2011; **30**: 79–89.

Supplementary Information accompanies the paper on European Journal of Human Genetics website (http://www.nature.com/ejhg)